Kaonic deeply bound states, the first experimental results

M. Iwasaki[a] for KEK PS-E471 collaboration

[a]DRI, RIKEN, Wako-shi, Saitama, 351-0198, Japan

Recently, we have performed an experimental search for deeply bound kaonic states by the kaon absorption reaction at rest in a liquid helium target. We observed very distinctive mono-energetic peak formation in a proton missing-mass spectrum. We denote it as a strange tribaryon, $S^0(3115)$, with baryon number 3, charge 0, isospin 1 and strangeness -1. If we attribute the mono-energetic peak to the formation of a deeply bound kaonic state, the separation energy of the kaon should be as deep as about 200 MeV. In the present paper, we will overview the present experimental data.

1 INTRODUCTION

Our knowledge of the interaction between the K-meson (especially $\overline{K}$) and the nucleus is far from satisfactory. Experimentally, the interaction has been studied either by the cross section of the in-flight $K^{\pm}N$ reaction, or the energy shift and broadening (due to the strong interaction) of the cascade x rays from kaonic atoms. The experimental approach is the same as πN, although the lower yield, shorter lifetime and the variety of reaction products make the kaon experiment much more difficult. Furthermore, the existence of the subthreshold resonance, $\Lambda(1405)$, 27 MeV below K^-p energy, makes the situation more complicated to understand.

Actually, x-ray data of kaonic hydrogen were puzzling for a long time because the x-ray observation and the subthreshold $\Lambda(1405)$ pole conflict. The strongly attractive nature between K^- and proton was confirmed recently[1]. There are two possible ways to understand the present experimental data; i) conventional optical-model calculations give a consistent result with the experimental data (excluding kaonic helium x-ray data) using an attractive but strongly absorptive interaction. On the other hand, ii) a coupled channel calculation by Akaishi and Yamazaki [2], in which the $\Lambda(1405)$ is treated as a bound state between K^- and proton, suggests that the $\overline{K}N$ interaction is extremely attractive and less absorptive, thus stable K-mesonic state formation is allowed in light nuclei.

Therefore, if we embed a kaon into the nucleus, a kaon is promptly absorbed by a nucleon (converted to a hyperon), in the former framework. On the other hand, in the latter framework, a kaon can survive longer than the typical time scale of the strong interaction, without loosing its identity as a meson in the nucleus. Thus, if one embeds a kaon into ^{3}He, a high density baryon system will be formed in which the kaon separation energy is as large as about 100 MeV with an absorption width of about 20 MeV.

The discovery of such a system will open a new research area to study hyper-dense matter in objects such as "compact stars", with densities greater than neutron stars, in the laboratory framework. In such a system, one may study the precursor effect toward the totally new $\langle \overline{q}q \rangle$-condensation phase, color super-conductivity, which may realize at the high density and low temperature limit. Because the constituent-quark or hadron mass is expected to be a function of $\langle \overline{q}q \rangle$-condensation strength, one may obtain a hint as to how hadronic mass is realized after the big bang. The quantum state of the bound kaon is well defined, so it will give us less ambiguous data compared to the high-density and high-temperature objects which can be realized in heavy ion collisions.

2 KEK PS-E471 EXPERIMENT

Very recently, we performed an experimental search for the predicted deeply-bound kaonic state by kaon absorption at rest in a liquid helium target. In the experiment, we observed nucleon emission from the reaction, and discovered distinct mono-energetic proton formation[3]. This can be produced by the two-body reaction of a proton together with the unknown object, S^0, whose mass is about 3115 MeV/c^2, namely,

$$(K^- \ ^4\mathrm{He})_{\mathrm{atomic}} \rightarrow \mathrm{S}^0(3115) + p. \qquad (1)$$

The observed system should have baryon number B=3, charge Z=0, isospin T=1 and strangeness $S = -1$.

The discovery of peak structure in the proton spectrum was quite astonishing to us, because we were searching for mono-energetic neutron formation. The theoretical prediction of a deeply-bound kaonic state by Akaishi and Yamazaki is the formation of the state at $M = 3194$ MeV/c^2 with $T = 0$ and $Z = 1$[2], which can only be studied via the

$$(K^- \ ^4\mathrm{He})_{\mathrm{atomic}} \rightarrow \mathrm{S}^+ + n \qquad (2)$$

reaction. Since the present experimental setup is not optimized for proton spectroscopy, we need to be very careful to check whether the proton peak in the spectrum has been formed for trivial reasons, such as experimental bias, other reaction processes, *etc.*

2.1 E471 Experimental Setup

Let us briefly describe our experimental setup, shown in Fig. 1. The negative kaon of 660 MeV/c is momentum degraded by a graphite block (not shown), its trajectory recorded by a fine segmented drift chamber (BDC), and stopped in the liquid ^{4}He target. We required at least one hit in the double-layered trigger counters (TC) to track one of the reaction/decay particles (mostly pions and protons) in a large area drift chamber (VDC). The pulse height information of the double-layered TC, together with injection angle obtained by VDC, enables us to perform a qualitative analysis of the p/π separation as shown in Fig. 2. A rough evaluation of the momentum can also be done if β is well below one, because the pulse heights are given by the partial integration of the Bethe-Bloch equation.

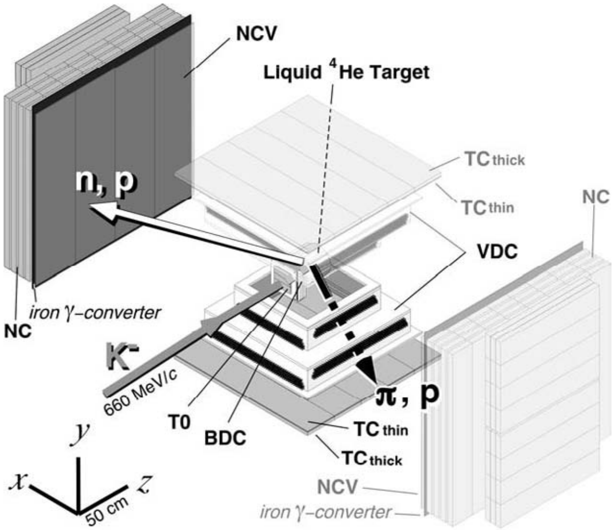

Figure 1: Schematic figure of the experimental setup. The notations are: T0, beam timing counter; BDC, beam-line drift chamber (16 layers); VDC, vertex drift chamber (12 layers); TC_{thin} and TC_{thick}, thin (0.6 cm) and thick (3 cm) trigger counter; NCV, neutron-counter charged-particle veto; NC, neutron-counter array (5 cm thick). Both tracking devices, BDC and VDC, are highly redundant to remove possible ghost tracks, important in the detailed vertex analysis. To simplify, several counters (mostly for veto) are omitted. All the scintillation counters shown here are viewed by PMTs at both ends.

The kaon reaction point is obtained by a closest-approach of the two trajectories between incoming kaon and outgoing reaction/decay particle. Kaon at-rest events in the target are selected by the correlation between the pulse height of the final beam line counter (T0 : placed between the degrader and the BDC) and the stopping range in the helium target.

The protons and neutrons are detected by a double-arm segmented plastic scintillator array (NC), which is placed 2 m away from the target center. A thin layer of scintillation counters (NCV) covering the NC array is for neutron separation for NC-detected particles, and p/π separation is done by using the energy sum of the NC array. The thin iron plate is to produce a γ-ray shower, which is used for the time-zero calibration of the NC array system. The momentum of the protons and neutrons is calculated by means of time-of-

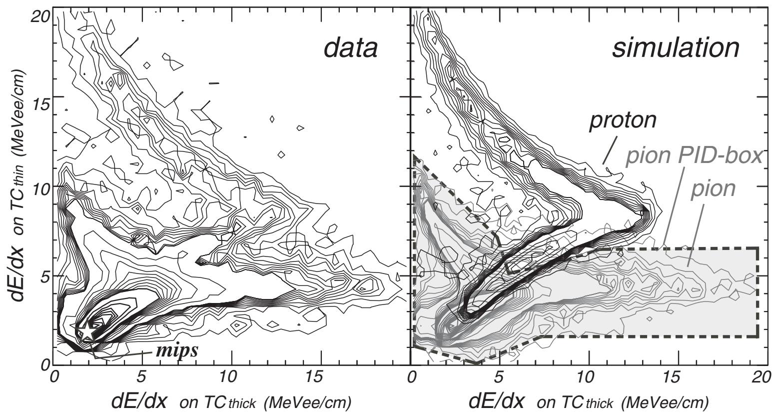

Figure 2: Contour plot of dE/dx on TC_{thick} (horizontal-) and TC_{thin} (vertical-axis) counters obtained by data (left). Minimum-ionizing-particles (*mips*) are expected to distribute around the star mark. In the simulation (right), proton- and pion-components are separately plotted, and the pion PID-box applied to the data is also shown as dashed line. The step of the contour is in logarithmic scale.

flight (TOF) from the reaction vertex to the detection point in the NC array.

2.2 Proton Spectrum

Fig. 3 shows the missing-mass spectrum of the protons obtained after the energy loss correction in the target. To demonstrate the stability of the particle identification (PID) boxes on the TC contour plot (shown in Fig. 2 (right)), we used slightly different PID criteria from those given in Ref. [3], in which the box shape is simplified with the resultant acceptance of high momentum proton contamination into the pions.

A clear signal is observed over the expected background protons, which mainly come from non-mesonic kaon absorption; $KNN \rightarrow \Lambda N$ (Br. ~ 20 %). We have studied all other possible experimental biases which may produce a fake peak in the spectrum, such as data comparison between left and right NC, and between the former and latter half of the data taking period, reaction-vertex fiducial cut, *etc.*

We requested a VDC-hit at the hardware level, so the missing mass spectrum is not an unbiased inclusive spectrum. One may wonder whether the trigger condition might bias the spectrum to form a spurious peak in the missing mass spectrum. However, it is impossible to form a peak structure because the angular acceptance in the x-y plane (the coordinate is shown in Fig. 1) is as large as $\pm$ 45^0, so that any kinematic bias should be smeared out.

As described in Ref. [3], the only possible background process is the chain reaction of

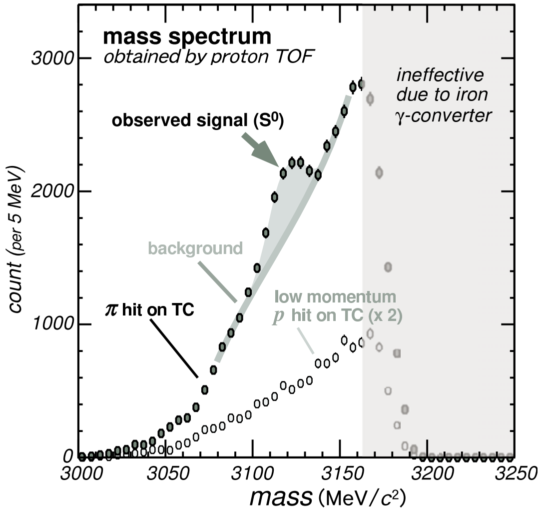

Figure 3: Missing mass spectrum of the semi-inclusive proton events. Close and open circle are for pion- and proton- triggered event on TC counter, respectively. The event-selection is obtained by the PID-box defined in Fig. 2.

hypernuclear formation and one of its non-mesonic decay branches

$$K^- + {}^4\mathrm{He} \rightarrow {}^4_\Lambda\mathrm{He} + \pi^- \quad (255\ \mathrm{MeV}/c) \quad \text{and} \tag{3}$$

$${}^4_\Lambda\mathrm{He} \rightarrow {}^3t + p \quad (508\ \mathrm{MeV}/c). \tag{4}$$

How about the yield of the peak formation? The hypernuclear formation probability is known to be about 2 %. On the other hand, the total non-mesonic decay branch is known to be about 16 %, but the partial branching ratio to the specific non-mesonic decay channel (4) is not known. The upper limit of the peak formation probability from this chain reaction is about 0.3 % per stopped kaon, and the actual branch could be one order of magnitude smaller. The yield is expected to be very small, however the momentum of a proton produced in reaction (4) is very close to that of the signal, so that one should be extremely careful.

In Ref. [3], we have already excluded this possibility by using the TC pulse height information. Actually, if the chain reaction (3) and (4) is the reason for peak formation, then the trigger particle on TC should be a pion from reaction (3), so that it is easy to check whether all the peak events are associated with the *minimum-ionizing-particles* (*mips*; the energy loss should be about 2 MeV/cm in both the $\mathrm{TC_{thin}}$ and $\mathrm{TC_{thick}}$ counter, marked as a star in Fig. 2). It is shown that the peak events are dominantly much slower than *mips* in the reference.

In the present paper, let's study the peak by a different approach. The tribaryon

$S^0(3115)$ is expected to be triggered mostly by the pion from the following decay chain,

$$S^0(3115) \rightarrow YNN \quad \text{and} \tag{5}$$
$$Y \rightarrow \pi^{\pm} N. \tag{6}$$

In this decay chain, the pion is produced by the weak decay of the hyperon (Y), then the motion of Y before the decay can be studied by the vertex inconsistency between incoming kaon and outgoing pion trajectories. Namely, in the formation process, the distance-of-closest-approach of the two trajectories may lie beyond the experimental vertex resolution because of hyperon motion. Moreover, the hyperon should be boosted opposite to the proton motion due to the formation reaction (1), so that the pion trajectory should reflect the boost.

To study this hyperon motion, let us introduce a scalar product $\mathbf{v}_{\mathrm{CA}} \cdot \hat{\mathbf{v}}_p$, where $\mathbf{v}_{\mathrm{CA}}$ is the vector from the kaon trajectory to that of the pion at the closest approach between the two trajectories, and $\hat{\mathbf{v}}_p$ is the unit vector of the proton motion. If vector $\mathbf{v}_Y$, which represents the hyperon track, is parallel to $\hat{\mathbf{v}}_p$, then $\mathbf{v}_Y$ is equal to $\mathbf{v}_{\mathrm{CA}}$ so that the scalar product $\mathbf{v}_{\mathrm{CA}} \cdot \hat{\mathbf{v}}_p$ gives the distance of the hyperon motion relative to the proton motion. Therefore, one can use the scaler product for the qualitative analysis of the motion of the hyperon relative to that of proton, although it looses sensitivity if the hyperon motion is orthogonal to $\hat{\mathbf{v}}_p$.

Fig. 4 shows the missing mass spectrum classified by $\mathbf{v}_{\mathrm{CA}} \cdot \hat{\mathbf{v}}_p$. The peak yield evaluation

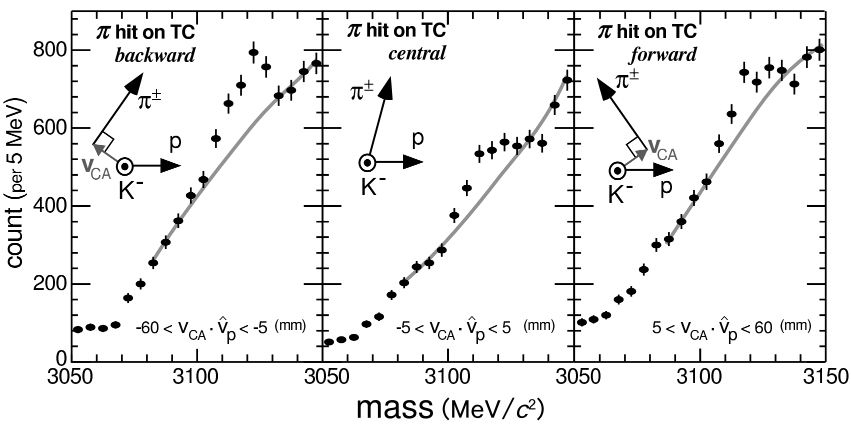

Figure 4: Missing mass spectrum of the pion triggered proton events, classified by three $\mathbf{v}_{\mathrm{CA}} \cdot \hat{\mathbf{v}}_p$ regions. $\mathbf{v}_{\mathrm{CA}} \cdot \hat{\mathbf{v}}_p$ regions and corresponding event topologies are shown as insets. The vertex in central $\mathbf{v}_{\mathrm{CA}} \cdot \hat{\mathbf{v}}_p$ region is consistent with the experimental vertex resolution.

in the three spectra is difficult because the background shape changes with $\mathbf{v}_{\mathrm{CA}} \cdot \hat{\mathbf{v}}_p$, and the lines in the spectra are simple spline functions with a node at 3200 MeV/c^2. It is clear that the function is not sufficient for the quantitative yield evaluation. However, the tendency is clear that the peak is mostly in the backward region, which is consistent with $S^0(3115)$ formation. On the other hand, if the peak is formed by the non-mesonic weak decay of the hypernucleus, reaction (3) ensures that the yield should be located dominantly in the central region.

2.3 Neutron Spectra

Fig. 5 (upper left) shows the semi-inclusive neutron spectrum. In contrast to the semi-inclusive proton spectrum, Fig. 3, it does not yield any distinct peak. Because recorded dE/dx information of the double-layered TC counters are the partial integration of the Bethe-Bloch equation, one can qualitatively classify events according to their trigger particles, namely "proton", "slow π ($p_\pi \lesssim 90$ MeV/c)" and "fast π ($p_\pi \gtrsim 125$ MeV/c)" triggered events, as shown in the figure.

A peak-like structure can be seen only in a "fast π" triggered event set. To study the neutron spectrum in more detail, let's focus on the hyperon motion using $\mathbf{v}_{\rm CA} \cdot \hat{\mathbf{v}}_n$ for this event set.

If the main decay channel of S^+ is similar to that of $S^0(3115)$, then one can assume that the ΣNN is the major decay channel, because pions from Σ decay have higher momenta than that from Λ decay. Thus one expects

$$S^+ \to \Sigma^\pm NN \ \text{ and } \ \Sigma^\pm \to \pi^\pm N, \tag{7}$$

which is an ideal model to apply the analysis procedure described above, because S^+ is expected to be boosted at the formation stage.

Fig. 6 shows the $\mathbf{v}_{\rm CA} \cdot \hat{\mathbf{v}}_n$ distribution of "fast π" triggered events having NC-detected neutron momenta $p_n > 400$ MeV/c. For a comparison, the decomposed spectra obtained by a simulation are shown.

As it is case in the proton spectra, shown in Fig. 4, the background spectrum of the neutron also depends on $\mathbf{v}_{\rm CA} \cdot \hat{\mathbf{v}}_n$. Therefore, we tried to interpolate the background shape using lower S/N (LSN : shallow hatched) regions to compare the event set of higher S/N (HSN : indicated with arrow) region. HSN is defined to be where we expect a better signal-to-noise ratio than in the other regions.

The missing-mass spectra both on HSN and LSN, obtained from the neutron data, are given in Fig. 7 (bottom). It shows that an enhancement exists at around the mass region from 3110 to 3160 MeV/c^2. As a comparison, we applied exactly same procedure to the proton data, as shown in Fig. 7 (top). We fitted the data of the HSN, assuming a smooth background for both the proton and neutron spectra. The fit for the proton HSN spectrum (background shape of a third-order polynomial was used) gave a consistent result with that obtained in a previous paper [3].

The excess in the neutron spectrum seems to be rather broad compared to that in the proton spectrum. It is natural to expect the isospin partner of $S^0(3115)$ in this energy region; hence, we fitted the HSN neutron spectrum with two Gaussian functions together with a smooth background (a single exponential), as shown in the figure, while fixing the mass and width of one Gaussian to be the same as that of $S^0(3115)$. In the fit, data of LSN were not utilized to constrain the background shape/yield.

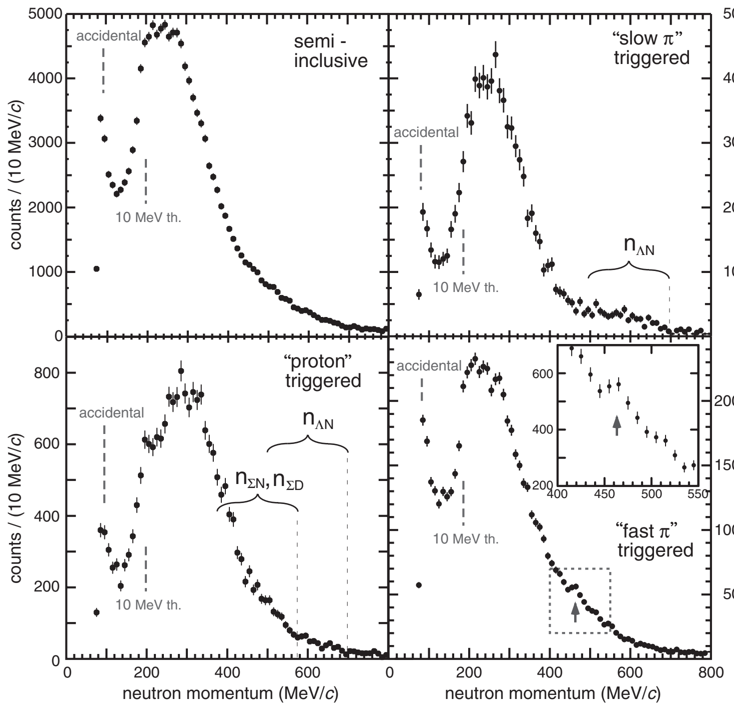

Figure 5: Neutron momentum spectra. The upper-left panel shows the semi-inclusive spectrum without any event selection, whereas the rest of the figures are subsets of the semi-inclusive spectrum using TC information. A peak-like structure exists in a "fast π" triggered event set at around $\sim$ 470 MeV/c; a close-up view of the doted region is given as an inset. $n_{\Sigma\mathrm{N}}$ and $n_{\Lambda\mathrm{N}}$ are for the neutron from kaon non-mesonic reaction ($K^-N \rightarrow \Sigma N$ and $K^-N \rightarrow \Lambda N$, respectively), and $n_{\Sigma\mathrm{D}}$ is for the neutron from Σ decay. The momentum regions of these reactions are shown in the figure.

The fit gave an energy of 3141 $\pm$ 3 MeV/c^2, width of 17 $\pm$ 5 MeV/c^2 and a yield of 120 $\pm$ 32 counts for the excess at the higher mass region. By folding the systematic error and the experimental resolution, we obtained a mass and width of M_{S^+} = 3141 $\pm$ 3 (stat.) $^{+4}_{-1}$ (*sys.*) MeV/c^2 and $\Gamma_{\mathrm{S}^+} < 23$ MeV/c^2 (95% *CL*), respectively. The significance of this excess, evaluated from the area of the Gaussian signal and its error, is 3.7 σ. The observed excess may indicate the formation of another strange tribaryon (denoted as $\mathrm{S}^+(3140)$), which lies about 25 MeV above $\mathrm{S}^0(3115)$.

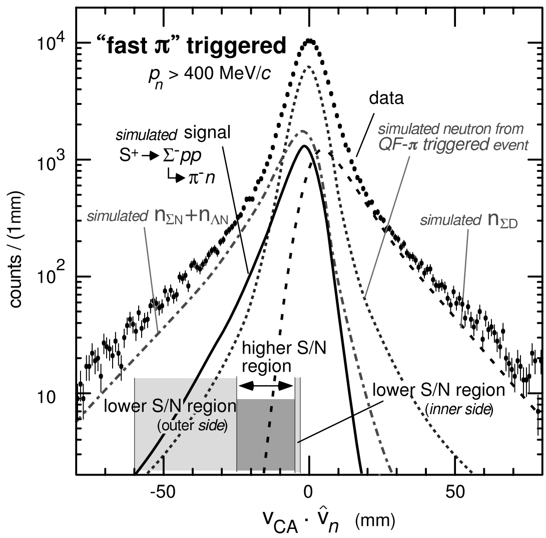

Figure 6: $\mathbf{v}_{\mathrm{CA}} \cdot \hat{\mathbf{v}}_n$ distribution. The dots with error bars show the data of the "fast π" triggered events associated with a high-momentum neutron ($p_n > 400$ MeV/c). The decomposition into key components, given by the simulation, is also shown. To make the signal formation component visible, the S^+ is simulated with a formation probability of 1% per stopped K^-0, and decays purely into $\Sigma^- pp$, which is the most efficient branch to detect in this $\mathbf{v}_{\mathrm{CA}} \cdot \hat{\mathbf{v}}_n$ selection.

3 CONCLUSION AND FORTHCOMING EXPERIMENTS

In the ^{4}He$(K^-, p)X$ reaction, we found very distinctive peak in the semi-inclusive proton spectrum, which we denoted as a strange tribaryon, $S^0(3115)$, with baryon number 3, charge 0, isospin 1 and strangeness -1.

On the other hand, in the neutron spectrum from ^{4}He$(K^-, n)X$ reaction, peak-like structure can only be seen when we selected "fast π" triggered event, which could be an indication of another tribaryon $S^+(3140)$. For more conclusive argument, we definitely need more statistics of the neutron data.

The nature of these peaks should be examined in the forthcoming experiments. There are two experimental programs, E549 and E570, scheduled in 2005 at KEK-K5 before the KEK PS shutdown. E549 is for more detailed study of the tribaryon $S^0(3115)$ by inclusive proton data using proton tracking device, and to achieve much more improved statistics for neutron data to study the candidate of $S^+(3140)$ using improved neutron shield and upgraded neutron counters.

E570 is to measure the kaonic helium x-ray transition from $3d$ to $2p$ to determine the

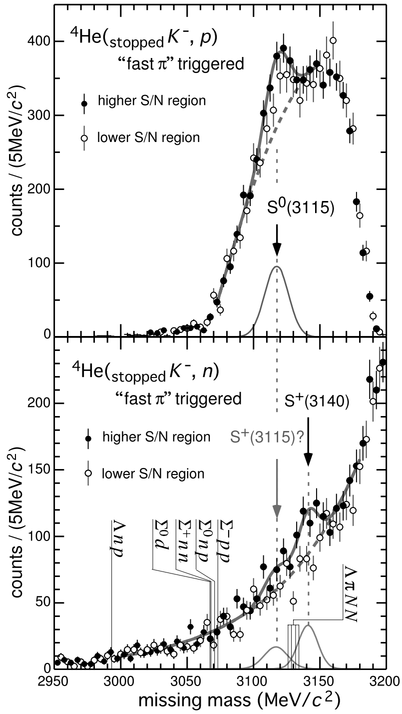

Figure 7: Missing-mass spectra of the ^{4}He($_{\rm stopped}K^-, p$) reaction (top) and the ^{4}He($_{\rm stopped}K^-, n$) reaction (bottom). Both proton and neutron HSN spectra were fitted assuming a smooth background. In the case of the HSN neutron spectrum (bottom), we couldn't achieved a good fit without assuming two Gaussian functions in the region of interest.

$\overline{K}N$ interaction. We are going to improve the statistics of neutron data using this beam period.

References

[1] M. Iwasaki et al., *Phys. Rev. Lett.* 78 (1997) 3067.

[2] Y. Akaishi and T. Yamazaki, *Phys. Rev.* C65 (2002) 044005.

[3] T. Suzuki et al., *Phys. Lett.* B597 (2004) 263.